

Simulation-based fatigue life assessment of a mercantile vessel

Ahmet H. Ertas^{*1} and Ahmet F. Yilmaz^{2,3}

¹Department of Biomedical Engineering, Karabuk University, Karabuk 78050, Turkey

²Department of Naval Architecture, Bartin University, Bartin 74100, Turkey

³Department of Mechanical Engineering, Karabuk University, Karabuk 78050, Turkey

(Received November 20, 2013, Revised April 15, 2014, Accepted April 24, 2014)

Abstract. Despite the availability of other transport methods such as land and air transportations, marine transportation is the most preferred and widely used transportation method in the world because of its economical advantages. In service, ships experience cyclic loading. Hence, it can be said that fatigue fracture, which occurs due to cyclic loading, is one of the most critical failure modes for vessels. Accordingly, this makes fatigue failure prevention an important design requirement in naval architecture. In general, a ship structure contains many structural components. Because of this, structural modeling typically relies on Finite Element Analysis (FEA) techniques. It is possible to increase fatigue performance of the ship structures by using FEA in computer aided engineering environment. Even if literature papers as well as rules of classification societies are available to assess effect of fatigue cracks onto the whole ship structure, analytical studies are relatively scarce because of the difficulties of modeling the whole structure and obtaining reliable fatigue life predictions. As a consequence, the objective of this study is to improve fatigue strength of a mercantile vessel against fatigue loads via analytical method. For this purpose, the fatigue life of the mercantile vessel has been investigated. Two different type of fatigue assessment models, namely Coffin-Manson and Morrow Mean stress approaches, were used and the results were compared. In order to accurately determine the fatigue life of the ship, a nonlinear finite element analysis was conducted considering plastic deformations and residual stresses. The results of this study will provide the designer with some guidelines in designing mercantile vessels.

Keywords: ANSYS; fatigue strength; Finite Element Analysis (FEA); mercantile vessel

1. Introduction

In general, the durability of a ship structure depends on its mechanical performance through its service life. Considering service, it can be said that damage is mainly due to fatigue in marine structures such as mercantile vessel shipboards and offshore platforms. Hence, in ship structures, the deformation mechanism under different types of loading have to be taken into account to design a safe and at the same time a reliable structure. In order to determine fatigue strength of a ship structure, accurate stress analysis and a systematic fatigue strength evaluation are needed. To evaluate fatigue strength and/or fatigue life values, different approaches such as the nominal stress

*Corresponding author, Ph.D., E-mail: ahertas@karabuk.edu.tr

approach (Ertas 2004, Pan 2000), the structural stress approach (Pan 2000), the notch stress approach (Pan 2000, Socie 1977), the notch strain approach (Pan 2000, Socie 1977, Peeker and Niemi 1999, Roessle and Fatemi 2000), volumetric fatigue approach (Pan 2000), and finally the crack propagation approach (Pan 2000) are used. The approach chosen depends on the method used to express fatigue strength data in the fatigue analysis (Wondseok *et al.* 2004).

There are numerous experimental or numerical studies related to marine based structures (Kim *et al.* 2012, Park and Lee 2012, Rizzo and Tedeschi 2007, Kozak and Gorski 2011, Fricke *et al.* 2012a, Fricke *et al.* 2012b, Fricke and Paetzold 2010, Suyuthi *et al.* 2013, Okawa and Sumi 2008, Kim *et al.* 2009, Sumi 1998, Cramer *et al.* 1995, White and Ayyub 1987). The important points of these studies can be summarized as follows:

Fricke and Paetzold (2010) conducted an experimental work. They have made tests considering full-scale ship structures. Using test results, they have also compared the experimental results with numerical ones. They used two different ship structures with five different loading. They have found that comparing with initiation, the propagation stages of the fatigue induced cracks were long. The correlation between experimental and numerical studies have been found satisfactory.

Suyuthi *et al.* (2013) have investigated ship hulls due to ice induced stresses. They generated a probabilistic procedure to estimate fatigue behavior of ship hulls taking into account the effect of iced waters. To do so, they considered three different statistical models, which are the one-parameter exponential, the Weibull's, and the three-parameter exponential models. Considering variation of ice thickness throughout the route, vessel's speed, and operational modes, they proposed a total fatigue damage accumulation for the hulls. They have found a close relation between fatigue life of the hulls considered and iced water as expected.

Okawa and Sumi (2008), on the other hand, have proposed a numerical approach for fatigue crack propagation in ship structures under clustered loading. In the proposed crack growth model, the authors have modeled the behavior of crack opening and closure by using the modified strip yielding model.

Kim *et al.* (2009), on the other hand, have compared hot spot stress and structural stress approaches for the fatigue assessment of a ship structure. Specifically, a fatigue strength assessment has been carried out for a side shell connection of a container vessel using both the hot spot stress and the structural stress methods and the results have been compared. When they have made this work, a consistent structural stress approach has been employed for the fatigue strength assessment of side-longitudinal stiffeners of an 8100 TEU container vessel. For the same structure, a fatigue strength assessment using the structural stress approach has also been carried out in order to compare with the hot spot stress method. They have found that the two methods have provided consistent results of fatigue life estimation within 10% difference. They also have found that T-type longitudinal stiffeners exhibit higher fatigue strength compared to that of L-type longitudinal stiffeners with some exceptions. At certain locations, it has been found that L-type longitudinal stiffeners exhibit higher fatigue strength under bending loads. In conclusion, for the fatigue strength assessment of ships, the structural stress approach has been found to be a viable alternative.

Sumi (1998) has investigated the essential features of fatigue crack propagation and the remaining life assessment for ship structures. He has also made a numerical analysis for the remaining life assessment of ship structures considering the effects of fatigue crack propagation and compared the numerical results with the experimental ones exist in the literature. He has found that the numerical results of crack paths and crack propagation lives were in good agreement with experimental results which means the method proposed can be applied to real crack propagation in the welded elements of ship structures.

Cramer *et al.* (1995) have summarized the fatigue life assessment approaches of ship structures and then proposed a methodology which estimates the accumulated fatigue damage under time varying loading via applied load vs. Number of cycles (S-N) fatigue approach assuming linear cumulative damage.

There are many different uncertainties related to fatigue life predictions. For example, the calculated loading on the ship structure is uncertain due to uncertainties in the wave climate description, the sailing state etc. The stress occurs in the ship is again uncertain due to uncertainties in the modeling and calculating local stress concentrations etc (Cramer *et al.* 1995). The fatigue life of a structure is uncertain due to uncertainties in the weld geometries, type and properties of weld material and size etc. These uncertainties has been led to probabilistic based fatigue analysis. White and Ayyub (1987), for example, have examined the reliability-based methods in the design of structures against fatigue. Then, they have proposed a new reliability-based fatigue assessment model for ship structures.

2. Fatigue life prediction models

Fatigue is one of the main failure mechanism for structures under cyclic loading. As a result considerable research has been carried out and progresses have been made in developing fatigue life prediction methodologies. Accordingly, there are a large number of models for fatigue life assessment proposed in the literature (Stephens *et al.* 2001, Suresh 2004, Cui 2002, Ong 1993). The afore mentioned approaches mainly can be divided into two parts which are Cumulative Fatigue Damage (CFD) and Fatigue Crack Propagation (FCP) based approaches. According to CFD approaches, fatigue damage increases with applied cycles in a cumulative manner, which may lead to fracture. Cumulative Fatigue Damage (CFD) theory is the traditional theoretical framework for Fatigue Strength Assessment (FSA). Fatigue Crack Propagation (FCP) theory, which is the most recent approach, based on fracture mechanics concepts (Fatemi *et al.* 1998). The details of the fatigue life prediction methods for metal structures can be found in reference (Cui 2002).

2.1 Cumulative Fatigue Damage (CFD) theories

Cumulative Fatigue Damage analysis plays a key role in predicting the life of components and structures subjected to field-load histories. Fatigue damage is fundamentally a result of material structural changes at the microscopic level, such as dislocations of the atomic structures. These macroscopic quantities can be used to account for crack nucleation and early growth. By choosing different macroscopic quantities such as stress, strain, energy density, or a combination of these, different cumulative fatigue damage formulas have been derived (Fatemi *et al.* 1998, Yang *et al.* 1998).

2.1.1 Stress-Based (S-N curve) approaches

The stress-based approach was the earliest, but is still the most frequently used, approach for fatigue life prediction. This approach is to base analysis on the nominal (average) stresses in the region of the component being analyzed. The nominal stress that can be resisted under cyclic loading is determined by considering mean stresses and by making adjustments for the effects of stress raisers, such as grooves, holes, fillets, and keyways. They involve empirical relations

between uniaxial fully reversed stress and fatigue life (S-N curves).

In this approach, the fatigue life (number of cycles N) is related to the applied stress range ($\Delta\sigma$ or S) or the stress amplitude (σ_a). In general, a plot of the fatigue life versus the true stress amplitude for a metal gives a curve of the Basquin form (Basquin 1910).

$$\sigma_a = \frac{E \cdot \Delta\varepsilon_e}{2} = \sigma'_f \cdot (2N)^b \quad (1)$$

where N is the number of cycles to failure, $2N$ is the number of load reversals to failure, σ'_f is the fatigue strength coefficient, and b is the fatigue strength exponent (the sign of b is negative).

In a component or structure, there are two types of stress concentration. One is due to the structural geometry change or discontinuity, and the other is due to welding. Depending on how the stress concentration effect is accounted for, stress-based approaches can be further divided into the nominal stress approach, the hot-spot stress approach, and the notch stress approach. Currently, the hot-spot stress approach seems to be the one most favored by ship classification societies (Wu *et al.* 2001, Hobbacher 2008). The mentioned relation (Eq. (1)) is valid for low cycle fatigue region. Recently, a new function to describe fatigue curves for both low and high fatigue regions, i.e., for the whole cycle region from tensile strength to fatigue limit, was proposed by Kohout and Vechet (Kohout *et al.* 1999). The function can be described as follow

$$\sigma(N) = \sigma_\infty \left[\frac{N + 10^7 \alpha \beta}{N + 10^7 \alpha} \right]^{-b} \quad \text{where } \alpha = \frac{\sigma_c^{-1/b} - \sigma_\infty^{-1/b}}{\sigma_u^{-1/b} - \sigma_\infty^{-1/b}} \quad \& \quad \beta = \frac{\sigma_u^{-1/b}}{\sigma_\infty^{-1/b}} \quad (2)$$

where σ_u is the tensile strength and σ_∞ is the fatigue limit, and both of them can be measured accurately. σ_c is the fatigue strength at 10^7 cycles and $-b$ is the slope in the middle of the cycle. σ_c and b can be determined by the least-squares method. Four parameters have to be determined for a complete S - N curve according to Eq. (2). Hence this function is not practical because all the necessary parameters may not be available.

2.1.2 Strain-Based approaches

According to these models, the range of values for strain controls the fatigue life. They also take into account the effect of plastic strain. They are, therefore, especially suitable for cases where plastic effects dominate the fatigue behavior. Although most engineering structures and components are designed such that nominal stresses remain elastic, stress concentrations often cause plastic strains to develop in the vicinity of notches, e.g., spot welds in our case. Fatigue cracks usually nucleate due to plastic straining at the notches. The total strain amplitude can be resolved into elastic and plastic strain components, each of which has been shown to be correlated with fatigue life via power-law relationships for most metals (Stephens *et al.* 2001). The total strain life equation (or modified Coffin-Manson relationship) relates alternating true elastic and plastic strains, $\Delta\varepsilon_e$ and $\Delta\varepsilon_p$, to fatigue life, that is the number of cycles to failure (N_f), as follows (Stephens *et al.* 2001, Suresh 2004).

$$\frac{\Delta\varepsilon}{2} = \frac{\Delta\varepsilon_e}{2} + \frac{\Delta\varepsilon_p}{2} = \frac{\sigma'_f}{E} (2N_f)^b + \varepsilon'_f (2N_f)^c \quad (3)$$

where σ'_f is the fatigue strength coefficient, ε'_f is the fatigue ductility coefficient, and b and c are

exponents determined by experiments.

In order to include the mean stress effect on fatigue life, several models were proposed in the literature. One method, often referred to as Morrow's mean stress method, replaces σ_f by $\sigma'_f - \sigma_m$ in Eq. (5), where σ_m is the mean stress (Stephens *et al.* 2001, Suresh 2004)

$$\frac{\Delta\varepsilon}{2} = \varepsilon_a = \frac{\Delta\varepsilon_e}{2} + \frac{\Delta\varepsilon_p}{2} = \frac{\sigma'_f - \sigma_m}{E} (2N_f)^b + \varepsilon'_f (2N_f)^c \quad (4)$$

An alternative version of this model where both the elastic and plastic terms are affected by the mean stress is given by (Stephens *et al.* 2001, Cui 2002)

$$\frac{\Delta\varepsilon}{2} = \varepsilon_a = \frac{\Delta\varepsilon_e}{2} + \frac{\Delta\varepsilon_p}{2} = \frac{\sigma'_f - \sigma_m}{E} (2N_f)^b + \varepsilon'_f \left(\frac{\sigma'_f - \sigma_m}{\sigma'_f} \right)^{c/b} (2N_f)^c \quad (5)$$

In the case of multi-axial stress and strain states, the equivalent alternating strain can be used (Stephens *et al.* 2001, Cui 2002, Ong 1993) in Eq. (5) assuming proportional loading using either the maximum principal strain

$$\varepsilon_{qa} = \varepsilon_{a1} \quad (6)$$

the maximum shear strain

$$\varepsilon_{qa} = \frac{\varepsilon_{a1} - \varepsilon_{a3}}{1 + \nu} \quad (7)$$

or the octahedral shear strain

$$\varepsilon_{qa} = \frac{\sqrt{(\varepsilon_{a1} - \varepsilon_{a2})^2 + (\varepsilon_{a2} - \varepsilon_{a3})^2 + (\varepsilon_{a3} - \varepsilon_{a1})^2}}{\sqrt{2}(1 + \nu)} \quad (8)$$

where ε_{a1} , ε_{a2} , and ε_{a3} are principal alternating strains with $\varepsilon_{a1} > \varepsilon_{a2} > \varepsilon_{a3}$ and ν is Poisson's ratio.

Another equation suggested by Smith, Watson, and Topper (often called the "SWT parameter") is given by (Stephens *et al.* 2001, Cui 2002, Roessle and Fatemi 2000)

$$\sigma_{\max} \varepsilon_a E = (\sigma'_f)^2 (2N_f)^{2b} + \sigma'_f \varepsilon'_f E (2N_f)^{b+c} \quad (9)$$

In order to save time and cost, it is often desirable to estimate fatigue life of a component or structure with a reasonable degree of accuracy using easily and quickly obtainable material properties such as hardness and tensile strength. Accordingly, many universally valid correlations between monotonic strength data and fatigue life have been proposed in the literature based on experimental data (Stephens *et al.* 2001, Roessle and Fatemi 2000). Among these relations, the Modified Universal Slopes method proposed by Muralidharan and Manson is the best known and given by (Stephens *et al.* 2001, Cui 2002, Roessle and Fatemi 2000)

$$\frac{\Delta\varepsilon}{2} = \varepsilon_a = 0.623 \left(\frac{S_{ut}}{E} \right)^{0.832} (2N_f)^{-0.09} + 0.0196 (\varepsilon_f)^{0.155} \left(\frac{S_{ut}}{E} \right)^{-0.53} (2N_f)^{-0.56} \quad (10)$$

where S_{ut} is the ultimate tensile strength. Another universal relation based on Brinell hardness (Roessle and Fatemi 2000) is given by

$$\frac{\Delta \varepsilon}{2} = \frac{4.25(HB) + 225}{E} (2N_f)^{-0.09} + \frac{0.32(HB)^2 - 487(HB) + 191000}{E} (2N_f)^{-0.56} \quad (11)$$

The final two approximations do not require coefficients or exponents specific to a material. They use only hardness, ultimate tensile strength, and modulus of elasticity (in MPa) for strain-life calculations; all of which are commonly available, or easily measurable. These equations are applicable to a range of materials.

2.1.3 Stress-based versus Strain-based approaches

The strain-based approach handles local plasticity effects in a more rational and detailed manner than does the stress-based approach. Hence, it is generally the preferred approach for analyzing short fatigue lives, as judged by the transition fatigue life of material, unless only rough estimates are needed. The strain-based approach can also be used at long lives where elastic strains dominate, in which case it becomes equivalent to a stress-based approach.

2.2 Fatigue Crack Propagation (FCP) theories

2.2.1 Long crack growth

The earliest theory for predicting the fatigue crack propagation length is the Linear Elastic Fracture Mechanics (LEFM) approach. The LEFM approach was first introduced by Paris and his colleagues (Paris *et al.* 1961) who equated fatigue crack growth rate to the cyclic elastic stress intensity factor range at the tip of a long crack subjected to a low value of cyclic stress, such that

$$\frac{da}{dN} = A(\Delta K)^n \quad \text{where } \Delta K = Y\Delta\sigma\sqrt{\pi a} \quad (12)$$

here A and n are material constants, and Y is a geometry factor depending on the loading and cracked body configuration,

Later, it has been found that the crack growth rate curve is not linear for all ranges of ΔK . There are three different regions in general which are initiation and threshold (region I), stable crack growth (region II), and unstable fracture (region III). In region I, the crack growth rate goes asymptotically to zero as ΔK approaches a threshold value ΔK_{th} . This means that for stress intensities below ΔK_{th} , there is no crack growth, i.e., there is a fatigue limit. The crack growth relations in the threshold region have been proposed as (Donahue *et al.* 1972)

$$\frac{da}{dN} = C \cdot [\Delta K - \Delta K_{th}]^m \quad (13)$$

Region II crack growth follows a power law, which is Paris–Erdogan crack growth law, (Paris *et al.* 1963) as given in Eq. (12).

Region III crack growth exhibits a rapidly increasing growth rate towards “infinity,” i.e., ductile tearing and/or brittle fracture. This has led to the relation can be given as follow (Foreman *et al.* 1967)

$$\frac{da}{dN} = \frac{C(\Delta K)^m}{(1-R)K_c - \Delta K} \quad (14)$$

where K_c represents the fracture toughness of the material.

Relations combining the departures from power-law behavior at high and low ΔK values also exist. The most representative one is probably the one proposed by McEvily and Groeger (McEvily *et al.* 1977).

$$\frac{da}{dN} = A(\Delta K - \Delta K_{th})^2 \left[1 + \frac{\Delta K}{K_c - K_{max}} \right] \quad (15)$$

2.2.2 Physically small crack growth

It is widely agreed that for physically small crack growth, the Elastic Plastic Fracture Mechanics (EPFM) must be employed. The EPFM approach was first introduced by Tomkins in 1968. Tomkins equated da/dN to crack tip decohesion to the bulk plastic strain field considering condition in the crack regime considered as follow (Paik *et al.* 2008)

$$\frac{da}{dN} = B(\Delta \varepsilon_p \sqrt{\pi a})^m - \text{Threshold condition in the crack regime} \quad (16)$$

On the other hand, McEvily and his colleagues (McEvily *et al.* 1977) proposed the following modified constitutive relationship for fatigue crack growth

$$\frac{da}{dN} = A \left\{ \left[\sqrt{\pi \gamma_e \left(\text{Sec} \frac{\pi}{2} \cdot \frac{\sigma_{max}}{\sigma_y} + 1 \right)} + Y \sqrt{\frac{\pi}{2} a \left(\text{Sec} \frac{\pi}{2} \cdot \frac{\sigma_{max}}{\sigma_y} + 1 \right)} \right] \Delta \sigma - (1 - e^{-ka})(K_{opmax} - K_{min}) - \Delta K_{effh} \right\}^2$$

$$\text{where } \gamma_e = \left(\frac{\Delta K_{effh}}{\Delta \sigma_{EL}} \right)^2 \cdot \frac{1}{\pi \left(\text{Sec} \frac{\pi}{2} \cdot \frac{\sigma_{max}}{\sigma_y} + 1 \right)} \quad (17)$$

here A is a material- and environment-sensitive constant (in $(\text{Mpa})^{-2}$), ΔK_{effh} is the effective range of the stress intensity factor at the threshold level (in $\text{MPa} \sqrt{m}$), K_{opmax} is the maximum stress intensity factor at the opening level for a macroscopic crack (in $\text{MPa} \sqrt{m}$), K_{min} is the minimum stress intensity factor applied (in $\text{MPa} \sqrt{m}$), k is a material constant which reflects the rate of crack closure development with crack advance, Y is a geometrical factor, a is the actual crack length (in m), σ_y is the yield strength of the material (in MPa), σ_{max} is the maximum stress applied (in MPa), and $\Delta \sigma_{EL}$ is the stress range of endurance limit (in MPa) (Paik *et al.* 2008).

2.2.3 Micro-structurally small crack growth

As the name imply micro-structural Fracture Mechanics (MFM) was developed to handle crack propagation at the micro-crack level. In MFM, the crack growth law is expressed as (Navarro *et al.* 1988)

$$\frac{da}{dN} = C \Delta \gamma^\beta (d - a) \quad (18)$$

where d and a represent the basal and real crack depths (as micro-structural dimensions), respectively.

2.3 Fatigue life for ship structures

If a structure contains highly localized regions, e.g., ship structures made of bulb flats, then stress-based approaches can be accepted as conservative because around the bulb flat connections can have highly localized plastic deformation. Hence, for fatigue life prediction of ship structures, use of strain-based approaches can be logical because they also include plastic strain effect in the analyses (Ertas *et al.* 2009). One of the strain-based models is the total strain life equation (or modified Coffin-Manson relationship) (Eq. (3)), which relates alternating true elastic and plastic strains, $\Delta\varepsilon_e$ and $\Delta\varepsilon_p$, to fatigue life, e.g., number of cycles to failure (N_f) (Stephens *et al.* 2001, Suresh 2004, Cui 2002, Ong 1993) explained above.

In order to include the mean stress effect on fatigue life, several models were proposed in the literature. One method, often referred to as Morrow's mean stress method, replaces σ_f by $\sigma_f - \sigma_m$ in Eq. (4).

3. Material and geometric properties

In ship building, basically five different steel, e.g., A, B, C, D, and E grade steels (Turkish Lloyd Rules 2013), are used. In this current study, Grade A type steel material has been chosen. Table 1 lists material properties of Grade A steel with yielding of 355 MPa. This material properties have been obtained experimentally. Table 2 (Ertas *et al.* 2014, Yilmaz 2013), on the other hand, shows geometric properties of the ship structure (barge) considered in this study. The so called properties were defined according to Turkish Lloyd Rules. Fig. 1 shows a typical mercantile vessel shipboard and amidship part with the coordinate system considered. In Fig. 1, x , y and z axes represent transverse axis (positive towards starboard side), longitudinal axis (positive towards forwards) and vertical axis (positive towards upwards), respectively. Origin, on the other hand, is located at the intersection of the longitudinal plane of symmetry of ship, the left end of length (L) and the baseline.

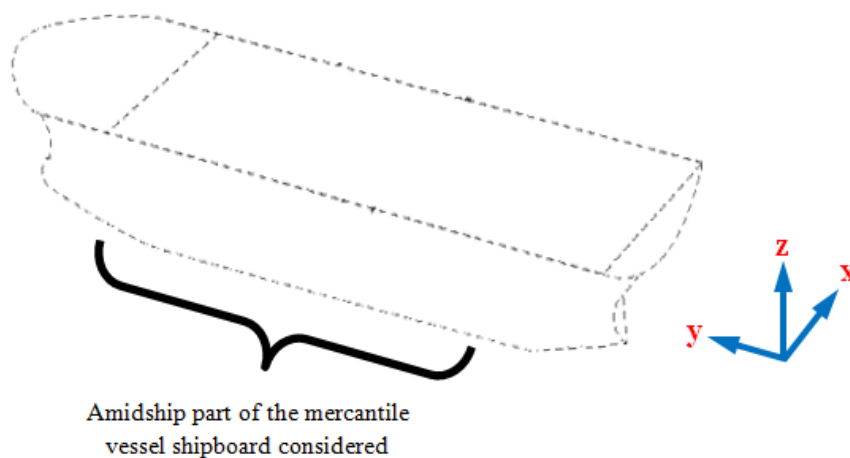


Fig. 1 A typical mercantile vessel shipboard and amidship part considered

Table 1 Material properties of Grade A type steel

Material property	Corresponding value
Young modules [GPa]	206
Poisson's ratio	0,3
Tensile Strength [MPa]	445
Yield Strength [MPa]	329
Average % elongation	37,5
Density [tone/mm ³]	7,85 10 ⁻⁹

Table 2 Geometric properties of the barge

Geometric property	Corresponding value
Full-length (L) [m]	135,8
Width (B) [m]	42
Depth [m]	8
Draft [m]	5,4
Block coefficient [C _B]	0,95
Barge speed [knot]	3
Wave coefficient [C _w]	6,4253
Service type coefficient	0,75
Length coefficient	1
$m = -C_{IH} / C_{IS}$	0,9944
Material factor	1
Class (Turkish Lloyd) (Turkish Lloyd Rules 2013)	TL

4. Fatigue life calculation

Fatigue life prediction models require accurate calculation of stress and strain states developed in the structure. For this purpose, commercial Finite Element Analysis (FEA) software, ANSYS (version 14), was used. Residual stresses developed during the formation of the shipboard were assumed not to affect the fatigue life and were not considered in the stress analysis. However, the residual stresses arising from non-uniform plastic deformations and developed after unloading were determined through the nonlinear stress analysis and considered. Dynamic effects were neglected and the load was assumed to be applied quasi-statically for this analysis.

In fatigue life calculation, off course the calculation or determination of the forces at sagging and hogging cases are very important. To define aforementioned forces, firstly a typical downright (vertical) shearing force has to be defined. Considering Turkish Lloyd Rules (Turkish Lloyd Rules 2013) a typical downright (vertical) shearing force can be calculated as follows

$$Q_{wv} = C_w \cdot C_B \cdot L \cdot B \cdot (C_B + 0.7) \cdot C_Q \quad (19)$$

Here, Q_{wv} represents the downright (vertical) shearing force; C_w , C_B , and C_Q represent wave coefficient, Moulded block coefficient and distribution factor, respectively. L and B represent length and breadth of the ship (in meters), respectively.

Wave coefficient (C_w) can be defined depending on the length of the ship (L) and service range coefficient (C_{RS}) as follows

Table 3 Service range coefficient (C_{RS})

Service condition	Corresponding value
For unlimited service range	1,0
For restricted service area (Y)	0,90
For restricted service area (K50)	0,75
For restricted service area (K20)	0,66
For restricted service area (L1 and L2)	0,60

Table 4 Distribution factor (C_Q)

Range	Positive shear force	Negative shear force
$0 \leq \frac{x}{L} < 0.2$	$1.38 \text{ m } \frac{x}{L}$	$-1.38 \frac{x}{L}$
$0.2 \leq \frac{x}{L} < 0.3$	0.276 m	-0.276
$0.3 \leq \frac{x}{L} < 0.4$	$1.104 \text{ m} - 0.63 + (2.1 - 2.76 \text{ m}) \frac{x}{L}$	$- [0.474 - 0.66 \frac{x}{L}]$
$0.4 \leq \frac{x}{L} < 0.6$	0.21	-0.21
$0.6 \leq \frac{x}{L} < 0.7$	$(3C_V - 2.1)(\frac{x}{L} - 0.6) + 0.21$	$- [1.47 - 1.8 \text{ m} + 3 (\text{m} - 0.7) \frac{x}{L}]$
$0.7 \leq \frac{x}{L} < 0.85$	$0.3 C_V$	$- 0.3 C_V$
$0.85 \leq \frac{x}{L} \leq 1.0$	$\frac{1}{3} [C_V (14 \frac{x}{L} - 11) - 20 \frac{x}{L} + 17]$	$-2 \text{ m} [1 - \frac{x}{L}]$

$$C_w = \begin{cases} 0.0857 L C_{RS} & \text{for } L < 90 \text{ m} \\ \left[10.75 - \left(\frac{300 - L}{100} \right)^{1.5} \right] C_{RS} & \text{for } 90 \text{ m} \leq L \leq 300 \text{ m} \\ 10.75 C_{RS} & \text{for } 300 \text{ m} < L < 350 \text{ m} \\ \left[10.75 - \left(\frac{300 - L}{150} \right)^{1.5} \right] C_{RS} & \text{for } 350 \text{ m} \leq L \leq 500 \text{ m} \end{cases} \quad (20)$$

Service range coefficient (C_{RS}) can be defined depending on the service conditions. For this parameter, the following table can be used.

Moulded block coefficient (C_B) at load draught T , and ship length, L , can be calculated as follows

$$C_B = \frac{V}{L.B.T} \quad (21)$$

where V represents moulded displacement at draught T (m^3). The draught T is the distance vertically at the middle of the ship from bottom (base) line to freeboard. C_{1H} and C_{1S} (in Table 2) are constants for Hogging and Sagging cases, respectively, and they are calculated depending on Moulded block coefficient (C_B) as follows

$$\begin{aligned} C_{1H} &= 0.19C_B \\ C_{1S} &= -0.11(C_B + 0.7) \end{aligned} \quad (22)$$

Table 5 Influence factor (C_V)

Service condition	Corresponding value
For undamaged condition	$\sqrt[3]{\frac{V}{1.4 \sqrt{L}}} \geq 1.0$
For damaged condition	1,0

Distribution factor (C_D) can be defined by using Table 4.

In Table 4, C_V is known as influence factor and can be defined as follows (Table 5).

5. Finite element model details

In the Finite Element (FE) model, SHELL181, was used for the ship structure. SHELL181 is suitable for analyzing thin to moderately-thick shell structures. It is a four-node element with six degrees of freedom at each node, that is translations in the x , y , and z directions, and rotations about the x , y , and z axes. SHELL181 is well-suited for especially linear and nonlinear, large deflection, large rotation, and/or large strain nonlinear applications. However, change in shell thickness is accounted for in nonlinear analyses. This element also has plasticity, creep, swelling and stress stiffening (ANSYS v14 2013).

Modeling the whole ship structure using solid elements leads to difficulties in meshing because this requires matching of the meshes of different parts. This adds enormously to the computational time. Additionally, to use solid elements for a shell shaped structures is also wrong from a conceptual viewpoint. For these reasons, SHELL181 was used. A typical ship structure (barge) mesh with focused one which were used for FEA were given in Fig. 2 (Yilmaz 2013). In Fig. 2, the numbers, e.g., 1, 2, 3, 4 and 5, show deep tank (water ballast), shell frame (Holland Profiles), forecandle bulkhead frames, watertight bulkhead and transition of stringer deck to shell stringer, respectively.

The boundary conditions in the FE model of the ship structure: In normal conditions, the symmetry conditions can be used, but this approach is valid just for linear static analysis. In this study, because of simplicity of ship structure due to shell elements and also accuracy of the results that were obtained using ANSYS package program, it was not used boundary symmetry conditions for 3-D finite element model of shipboard. Additionally, nonlinearity exists due to plastic deformations and contact portions of the structure. So, it is not reasonable to apply symmetry conditions arbitrarily, including both geometry symmetry wherever possible in order to decrease model size and loading symmetry.

Displacements and rotations in vertical axis (the z -direction) (see Fig. 1 for coordinates) at the bottom plate of the barge structure were fixed. The upper deck of the barge was subject to uniformly distributed in-plane load cycle in the z -direction, that is vertical axis (positive towards upwards), while the movement is not prevented in the other degrees of freedom. The details of the FE model of the mercantile vessel considered can be found in references (Ertas *et al.* 2014, Yilmaz 2013). Fig. 3 shows the simulation procedure for the study.

The cyclic loading was applied in two load steps. First, the load was incrementally increased to its maximum value, P_{\max} , and the resulting stress state was obtained. In the second load step, the

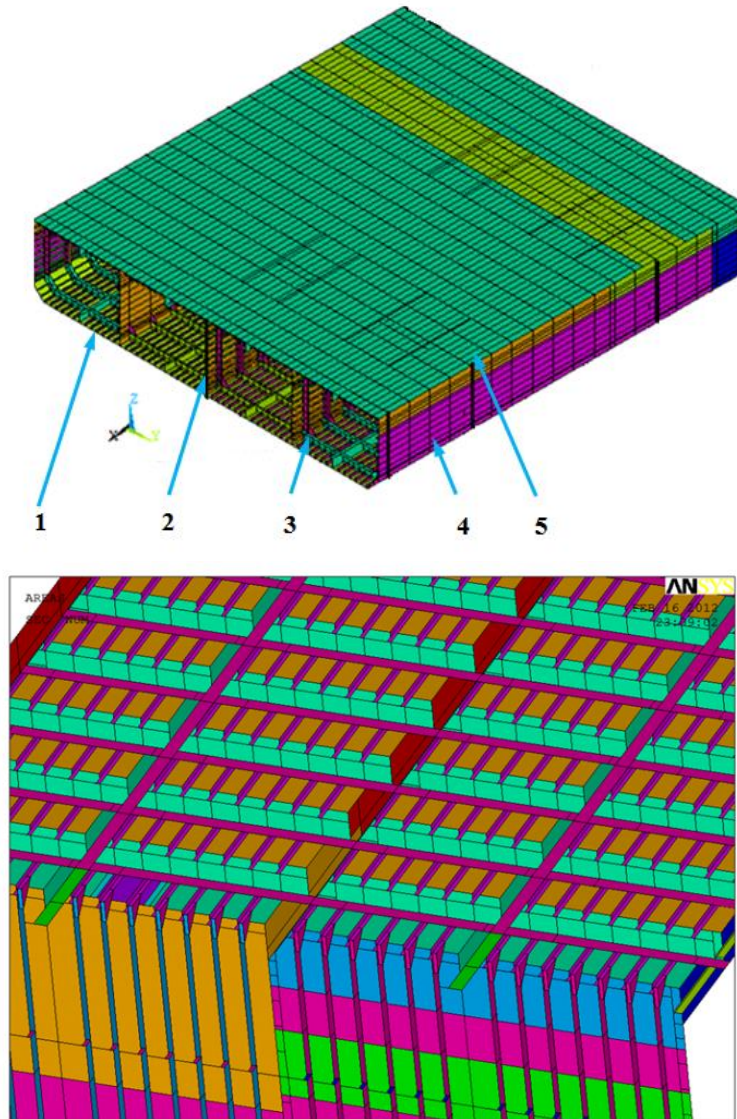


Fig. 2 Typical amidship structure (barge) mesh used for FEA

load was incrementally decreased to its minimum value, P_{\min} . In the next load cycles, stresses were assumed to fluctuate between the stress values obtained for the maximum and minimum load levels in the first load cycle. In both cases program found the most critical regions and used the corresponding stress and strain values in fatigue life calculations.

Using data from “fatigue life calculation” obtained for the vessel structure considered, the distribution factors and the corresponding vertical wave shear forces for hogging and sagging are given in Table 6.

Figs. 4 and 5 show (Ertas *et al.* 2014, Yilmaz 2013) the distributions of von Mises stress and total strain values, respectively developed after the maximum sagging (16099,47 kN) and hogging

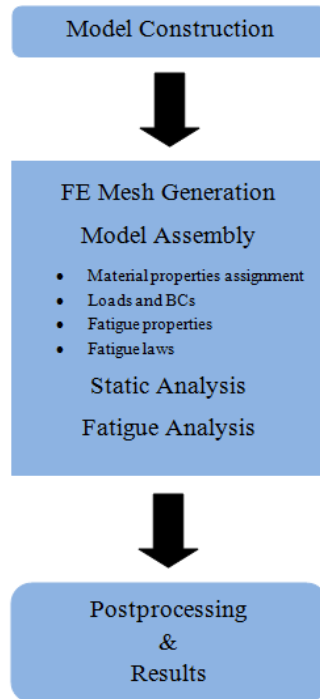


Fig. 3 Simulation procedure

Table 6 Distribution factors and the corresponding vertical wave shear forces

Range (m)	C_Q for Sagging	C_Q for Hogging	Q_{wv} for Sagging (kN)	Q_{wv} for Hogging (kN)
7.5	0.078	0.078	4608.62	-4583.23
28.75	0.274	0.276	16099.47	-16188.67
42.5	0.259	0.261	15243.25	-15312.25
66	0.210	0.210	12317.46	-12317.46
85	0.238	0.114	13968.92	-6740.26
100	0.272	0.298	15964.76	-17499.43
118.75	0.146	0.195	8617.30	-11492.17

(4583,23 kN) loads were applied. As seen in high stresses developed at the connections between metal sheet and bulb flats.

Because the minimum load is low compared with the maximum load, significant compressive stresses existing after unloading may only be attributed to residual stresses developed due to non-uniform plastic deformation. Because stiffeners, e.g. bulb flats, are exposed to bending due to working condition of ship structures, bending induces larger stresses. Due to the effect of bending, stresses change from tension to compression through the thickness of body sheet. For this reason, flexural rigidity of the plate, i.e., its resistance to bending significantly affects the stress level even though the parts of the structures are subject to in-plane loading. Considering also that the load is transferred through the joints, one may see why stresses are more concentrated in the joints (Fig. 4).

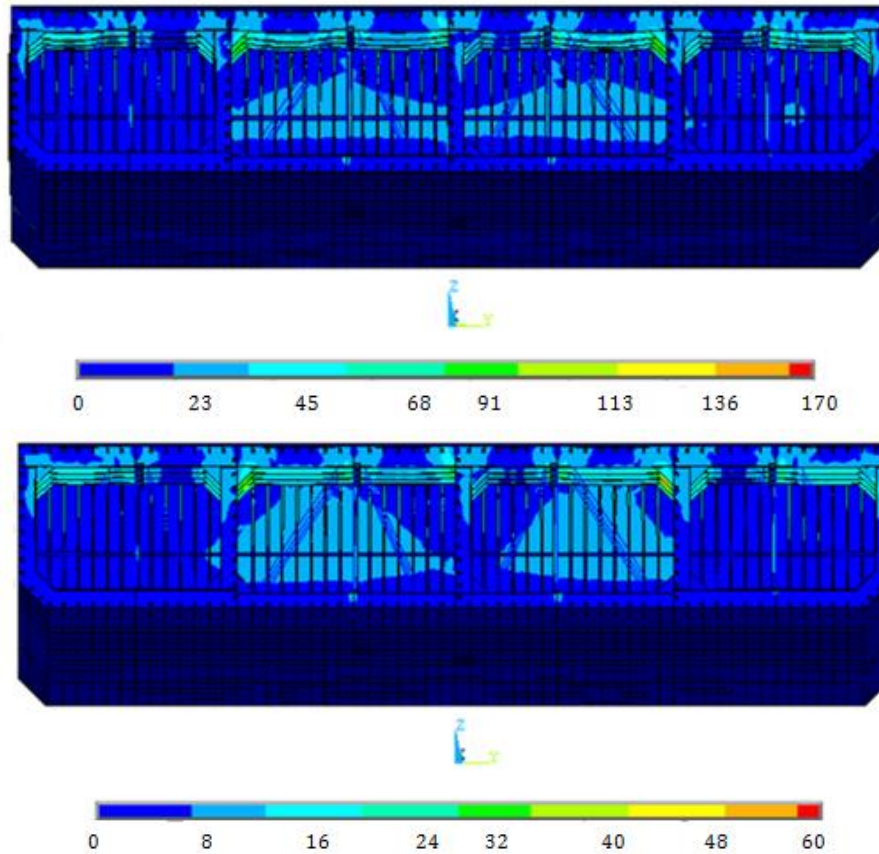


Fig. 4 von Mises stress distribution of the amidship structure for sagging and hogging cases

When the location of the point where the maximum stress developed was examined, this point was observed to become closer to the joint or connections of bulb flats and metal sheets with the decreasing load range. This conformed to the trend that crack initiation sites were closer to the connections for low loads. The reason why the maximum stress develops at a farther distance from the connections with a larger load may be attributed to an enlarged yield zone away from the connections.

6. Assessment of FE analysis

As seen in Figs. 4 and 5, load transfer in the ship structure (barge) is mainly accomplished by the material near the boundary of the stiffeners, bulb flats (Holland profiles) while the rest of the structure is mostly stress-free which proof why the designs of stiffeners in a ship structure are important. Also this proofs why notch based fatigue life prediction approaches are valid for a whole ship structure. Also, it is clear from the FE Analysis that a stress concentration or singularity exists at the interception of the bulb flats with the joined sheets because all von Mises stresses have their maximum magnitudes at the so called regions. These stress distributions also

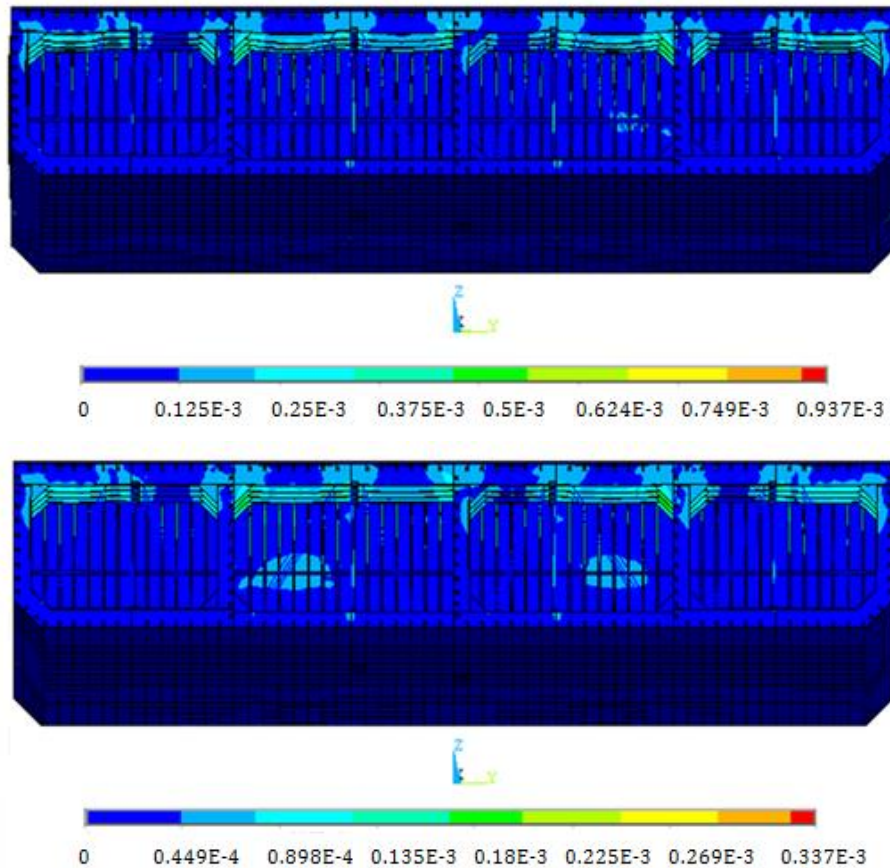


Fig. 5 Total strain distribution of the amidship structure for sagging and hogging cases

explain successfully the phenomenon that why the fractures are generally first created at the connections of bulb flats and ship shell plates.

The fatigue life of the ship structure was estimated using the available fatigue assessment models which are Coffin-Manson and Morrow's mean stress approaches. In order to apply the models, which account for fatigue failure only in uniaxially loaded parts, we need to find equivalent stress and strain values representing the multi-axial stress and strain states that developed in the ship structure. There are mainly three approaches: The maximum principal strain, the maximum shear strain, and the octahedral shear strain. Because the octahedral shear strain and the maximum principal strain better represent the effect of multi-axial strain state (Stephens *et al.* 2001), the octahedral shear strain was used in the fatigue life calculations.

The fatigue lives were calculated based on the stress and strain states at the point where the maximum tensile stress developed. Alternatively, the points where the maximum shear stress or Von Mises stress developed were also tried. However, non-conservative predictions were obtained for high cycle fatigue. Thus, the criterion initially adopted to determine the critical point turned out to be appropriate. Figs. 6 and 7 show the load range vs. number of cycles to failure of the ship structure according to Coffin-Manson and Morrow's mean stress approaches respectively.

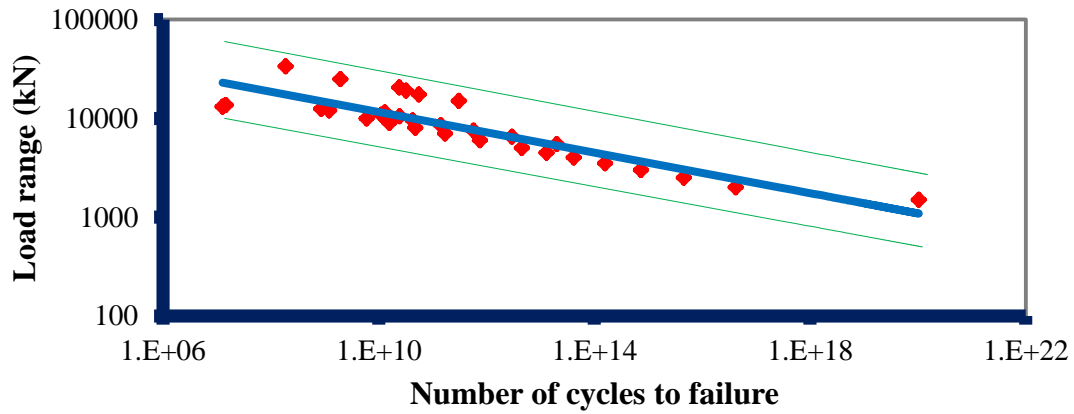


Fig. 6 Fatigue lives predicted using modified Coffin-Manson approach

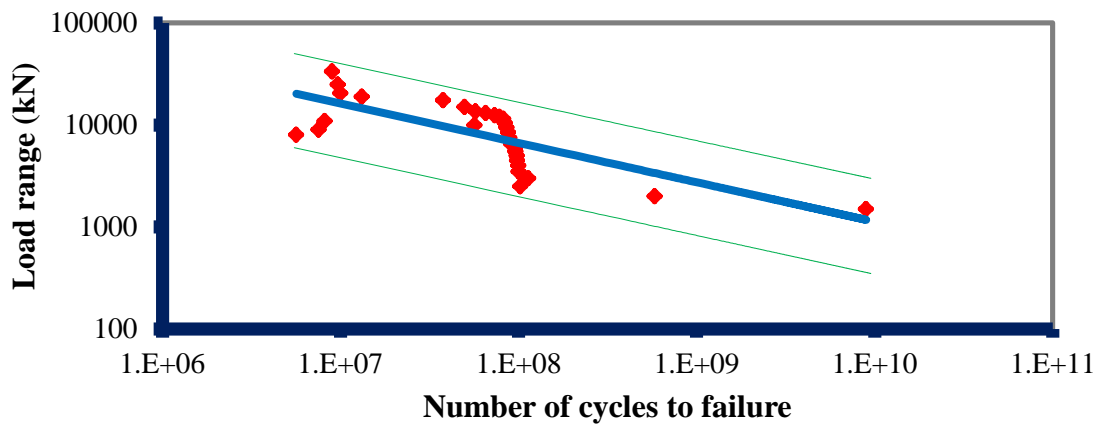


Fig. 7 Fatigue lives predicted using Morrow's mean stress approach

7. Conclusions

In this study the fatigue failure behavior of a ship structure (barge) was investigated numerically. FE analyses were carried out taking into account nonlinear constitutive relations, plastic deformation, and residual stresses to determine the stress and strain states in the structure under cyclic loading. High stresses were found to develop close to highly localized regions, e.g. ship structures made of bulb flats. The reason why the maximum stress develops at a farther distance from the connections with a larger load may be attributed to an enlarged yield zone away from the connections.

The fatigue lives of the structure was estimated using the available general purpose fatigue failure models. Because the stress state in the structure was multiaxial and the fatigue models were structured for uniaxially stressed parts, equivalent stress or strain approaches were adopted. Among them, Von Mises stress and maximum principal strain (or octahedral shear strain) were found to better reflect the effect of multiaxial strain and stress states. The fatigue life predictions of

stress-based approaches were overly conservative. Among the strain-based approaches, Coffin - Manson and Morrow's mean stress models yielded the best correlations. These models can reliably be used in designing ship structures.

Acknowledgments

The authors wish to express their thanks to Dr. Veysel Alkan for his helpful comments.

References

- ANSYS (2013), ANSYS Documentation, v.14, UK.
- Basquin, O.H. (1910), "The exponential law of endurance tests", *Proc. ASTM*, **10**, 625-630.
- Cramer, E.H., Loseth, R. and Olaisen, K. (1995), "Fatigue assessment of ship structures", *Mar. Struct.*, **8**, 359-383.
- Cui, W.C. (2002), "A state of the art review on fatigue life prediction methods for metal structures", *J. Mar. Sci. Technol.*, **70**(1), 43-56.
- Donahue, R.J., Clark, H.M. and Atanmo, P. (1972), "Crack opening displacement and the rate of fatigue crack growth", *Int. J. Fract. Mech.*, **8**, 209-219.
- Ertas, A.H. (2004), "Fatigue behavior of spot welds", M.Sc. Thesis, Bogazici University, Istanbul.
- Ertas, A.H., Alkan V. and Yilmaz A.F. (2014), "Finite element simulation of a mercantile vessel shipboard under working conditions", *Procedia Eng.*, **69**, 1001-1007.
- Ertas A.H., Vardar O., Sonmez F.O. and Solim Z. (2009), "Measurement and assessment of fatigue life of spot-weld joints", *J. Eng. Mater-T ASME*, **131**, Article Number: 011011.
- Fatemi, A. and Yang, L. (1998), "Cumulative fatigue damage and life prediction theories: a survey of the state of the art for homogeneous materials", *Int. J. Fatigue*, **20**, 9-34.
- Foreman, R.G., Kearney, V.E. and Engle, R.M. (1967), "Numerical analysis of crack propagation in cyclic-loaded structures", *J. Basic Eng.*, **89**, 459-464.
- Fricke, W. and Paetzold, H. (2010), "Full-scale fatigue tests of ship structures to validate the S-N approaches for fatigue strength assessment", *Mar. Struct.*, **23**(1), 115-130.
- Fricke, W., von Lilienfeld-Toal, W. and Paetzold, H. (2012a), "Fatigue strength investigations of welded details of stiffened plate structures in steel ships", *Int. J. Fatigue*, **34**(1), 17-26.
- Fricke, W., Zacke, S., Kocak, M. and Eren, S.E. (2012b), "Fatigue and fracture strength of ship block joints welded with large gaps", *Weld. World*, **56**(3-4), 30-39.
- Hobbacher, A. (2008), *Recommendations for fatigue design of welded joints and components*, International Institute of Welding.
- Kim, M.H., Kim, S.M., Kim, Y.N., Kim, S.G., Lee, K.E. and Kim, G.R. (2009), "A comparative study for the fatigue assessment of a ship structure by use of hot spot stress and structural stress approaches", *Ocean Eng.*, **36**(14), 1067-1072.
- Kim, D.K., Park, D.K., Seo, J.K., Paik, J.K. and Kim, B.J. (2012), "Effects of low temperature on mechanical properties of steel and ultimate hull girder strength of commercial ship", *Korean J. Met. Mater.*, **50**(6), 427-432.
- Kohout, J. and Vechet, S. (1999), "New functions for a description of fatigue curves and their advantages", *Proceedings of the 7th International Fatigue Congress (Fatigue'99)*, Eds. Wu, X.R. and Wang, Z.G., Higher Education Press, Beijing.
- Kozak, J. and Gorski, Z. (2011), "Fatigue strength determination of ship structural joints Part I Analytical methods for determining fatigue strength of ship structures", *Pol. Marit. Res.*, **18**(2), 28-36.
- McEvily, A.J. and Groeger, J. (1977), "On the threshold for fatigue-crack growth", *Proceedings of the 4th*

- International Conference on Fracture*, **2**, University of Waterloo Press, Waterloo, Canada.
- Navarro, A. and De los Rios, E.R. (1988), "A microstructurally short fatigue crack growth equation", *Fatig. Fract. Eng. Mater. Struct.*, **11**, 383-396.
- Okawa, T. and Sumi, Y. (2008), "A computational approach for fatigue crack propagation in ship structures under random sequence of clustered loading", *J. Mar. Sci. Tech-Japan*, **13**(4), 416-427.
- Ong, J.H. (1993), "An evaluation of existing methods for the prediction of axial fatigue life from tensile data", *Int. J. Fatigue*, **15**(1), 13-19.
- Paik, J.K. and Melchers, R.E. (2008), *Condition assessment of aged structures*, Woodhead Publishing in Mechanical Engineering, CRC Press, USA.
- Pan, N. (2000), "Fatigue life study of spot welds", Ph.D. Dissertation, Stanford University, San Francisco.
- Paris, P.C. and Erdogan, F. (1963), "A critical analysis of crack propagation laws", *J. Basic Eng.*, **85**, 528-534.
- Paris, P.C., Gomez, M.P. and Anderson, W.P. (1961), "A rational analytical theory of fatigue", *Trend. Eng.*, **13**, 9-14.
- Park, S.J. and Lee, H.W. (2012), "A study on the fatigue strength characteristics of ship structural steel with gusset welds", *Int. J. Nav. Arch. Ocean Eng.*, **4**, 132-140.
- Peeker, E. and Niemi, E. (1999), "Fatigue crack propagation model based on a local strain approach", *J. Constr. Steel Res.*, **49**(2), 139-155.
- Roessle, M.L. and Fatemi, A. (2000), "Strain-controlled fatigue properties of steels and some simple approximations", *Int. J. Fatigue*, **22**(6), 495-511.
- Rizzo, C.M. and Tedeschi, R.A. (2007), "Fatigue strength of a typical ship structural detail: tests and calculation methods", *Fatig. Fract. Eng. M.*, **30**(7), 653-663.
- Socie, D.F. (1977), "Fatigue-life prediction using local stress strain concepts", *Exp. Mech.*, **17**(2), 50-56.
- Stephens, R.I., Fatemi, A., Stephens, R.R. and Fuchs, H.O. (2001), *Metal Fatigue in Engineering*, Wiley-Interscience Publication, New York, NY, USA.
- Sumi, Y. (1998), "Fatigue crack propagation and computational remaining life assessment of ship structures", *J. Mar. Sci. Technol.*, **3**(2), 102-112.
- Suresh, S. (2004), *Fatigue of Materials*, Cambridge University Press, Cambridge, UK.
- Suyuthi, A., Leira, B.J. and Riska, K. (2013), "Fatigue damage of ship hulls due to local ice-induced stresses", *Appl. Ocean Res.*, **42**, 87-104.
- Turkish Lyod Rules (2013).
- White, G.J. and Ayyub, B.M. (1987), "Reliability-based fatigue design for ship structures", *Nav. Eng. J.*, **99**(3), 135-149.
- Wondseok, J., Bae D. and Sohn, I. (2004), "Fatigue design of various type spot welded lap joints using the maximum stress", *KSME Int. J.*, **18**(1), 106-113.
- Wu, Y.S., Cui, W.C. and Zhou, G.J. (2001), *Practical Design of Ships and Other Floating Structures*, Elsevier, Shanghai, September.
- Yang, L. and Fatemi, A. (1998), "Cumulative fatigue damage mechanisms and quantifying parameters: a literature review", *J. Test Eval.*, **26**(2), 89-100.
- Yilmaz, A.F. (2013), "Fatigue analysis of the ship structure made of Holland profiles", M.Sc. Thesis, Karabuk University, Karabuk, Turkey. (in Turkish)